Electronic Supplementary Material (ESI) for Journal of Materials Chemistry B.
This journal is © The Royal Society of Chemistry 2014

Supporting Information

Anti-photobleaching flower-like microgels as optical nanobiosensors with high selectivity at physiological condition for continuous glucose monitoring

Xinjie Zhang[a], Chunmei Gao[a], Shaoyu Lü[a], Haogang Duan[a, b], Nannan Jing[a], Di Dong[a], Caifeng Shi[a], Mingzhu Liu[a]*

[a] State Key Laboratory of Applied Organic Chemistry and Department of Chemistry, Key Laboratory of Nonferrous Metal Chemistry and Resources Utilization of Gansu Province, Lanzhou University, Lanzhou 730000, P.R. China

[b] Pharmacy Department of First hospital, Lanzhou University, Lanzhou 730000, P.R. China

* Corresponding author Tel: +86-931-8912387; fax: +86-931-8912582

E-mail address: mzliu@lzu.edu.cn

Characterization

Micrographs of the microgel were conducted on a JEM-1200EX/S (Hitachi, Japan) transmission electron microscope (TEM) operating at an accelerating voltage of 200 kV. The samples for TEM observations were prepared by evaporation of the prepared solution on a formvar coated copper grid. Scanning electron microscope (SEM) (JSM-5600 LV SEM, Japan) was applied to observe the microgels. Samples for SEM determination were also prepared by slow evaporation of the designed solution on an aluminum grid and sputter-coated with gold for 60 s. Fluorescent images with designed concentration of microgels were recorded on Fluorescence microscope (Olympus, Japan). Transmitting polarized microscope XS-402P (POM) was applied to observe morphology of microgels. Phosphorescence spectrophotometer (LS 55, Perkin Elmer Co., USA) was taken to record fluorescence spectra at the excitation wavelength of 360 nm under room temperature. 15 nm was set as slit widths for both excitation and emission. For all fluorescence measurements of microgel dispersion were fixed at 1.0×10^{-5} g/mL.

***In Vitro* Cytotoxicity Measurement**

Cell viability was assayed with respect to HeLa cells by the MTT assay. The cells were cultured in DMEM with 10% of fetal bovine serum (FBS) and a humidified atmosphere (5% CO_2, 37°C). HeLa cells were seeded in a 96-well plate at an initial density of 7000 cells/well and further incubated with 100 μL fresh medium. Microgel dispersions were sterilized by autoclave and then added to achieve varying final concentrations. After incubation for 24 h at 37°C， MTT reagent (10 μL in PBS, 5 mg/mL) was added to each well for further 4 h incubation at 37°C. Then, the culture medium was removed and replaced with 100 μL DMSO to dissolve the formed formazan crystals. Untreated cells which were taken as control had 100% viability (%) that correlates with amount of liable cells compared with cell control. Each experiment repeated five times. The data were shown as the mean value plus a standard deviation (± SD).

Evaluation of fluorescent ability *in vitro* and *in vivo*

Confocal laser scanning microscopy (CLSM) was employed to investigate whether incubation with cells would have effect on glucose detection. Firstly, the HepG2 cells were seeded in a glass base dish with a coverslip at a density of 5×10^4 cells and cultured for 24 h. Then 0.1 mg/mL microgels were added, and cells were cultured under designed glucose concentrations for 0.5 h in a humidified 5% CO_2-containing atmosphere. Finally, the location of intracellular fluorescence was validated using a CLSM imaging system (LYMPUS FV-1000) at the excitation wavelength of 360 nm.

The evaluation of transdermal detection *in vivo* was done with KM mice. The mice (4 weeks, 18~22 g) were cared in accordance with international standards on animal welfare and the Animal Research Committee of the University. The ability to emit light from skin of the portions of the mice ears with and without the fabricated microgels was investigated under 365 nm UV light and photos were taken by digital camera. Briefly, we performed tests on five mice, each mouse was injected 0.1 mL 1 mg/mL microgel solution by injection syringe (Gauge 26 G) under the skin of mouse's ear. After that, the mouse was put under UV light (4W, WFH-203 tri-use UV analyzer, Shanghai Jinke industrial co., ltd).) with 365 nm excited wavelength in the dark room. Photos were taken by the Sony (DSC WX 220) digital camera.

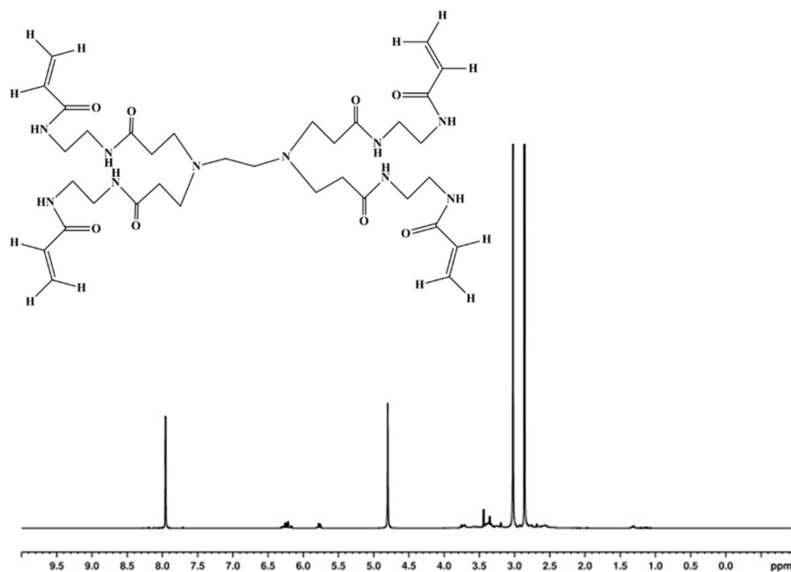

Fig. S1 ^{1}H NMR of acryl-functionalized G1.0 PAMAM

^{1}H NMR (400 M, D_2O, δ ppm)

δ 2.85 (N$\mathit{CH_2}\mathit{CH_2}$N), δ 3.05 (N$CH_2\mathit{CH_2}$CONH), δ 3.20 (NH$CH_2\mathit{CH_2}$NH), δ 3.40 (N$\mathit{CH_2}CH_2$CNHC$\mathit{H_2}$NH), δ 5.75 , 6.25 (COC$\mathit{H}C\mathit{H_2}$), δ 8.0 (CON$\mathit{H}CH_2CH_2N\mathit{H}$)

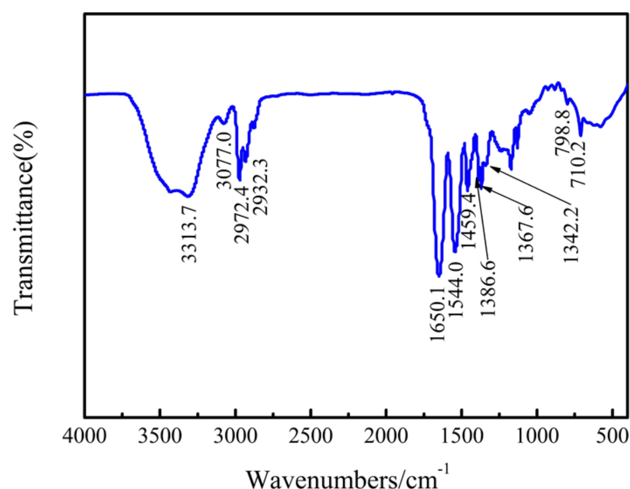

Fig. S2 FTIR spectra of fabricated microgel.

Fig. S2 shows the FTIR spectra of fabricated microgel. In Fig. S2, 3077 cm^{-1} is typical absorption of C-H stretching vibration of benzene. The characteristic bands occurred in the fingerprint region at 710 and 798 cm^{-1} means it is a meta-benzene. Besides, 1342 cm^{-1} absorption is characteristic peak of $–B(OH)_2$. Based on these data, it can be confirmed that AAPBA has been successfully fabricated in the microgel. Despite the introducing of AAPBA, PNIPAM and PDMAEMA also have been introduced in the microgel. The peaks at 2972 and 2932 cm^{-1} are assigned to asymmetric stretching vibration of CH_3 and CH_2, respectively. 1650 and 1544 cm^{-1} appear typical absorption of amide Ⅰ and amide Ⅱ in PNIPAM. Besides, the absorption band at 1173 cm^{-1} is attributed to C-O-C asymmetric stretching vibration of PDMAEMA. Despite the characteristic peaks of PAAPBA, PNIPAM and PDMAEMA, 3313 and 1650 cm^{-1} are characteristic absorption of N-H and C=O stretching vibration, indicating the introduction of G 1.0 PAMAM.

Despite FTIR analysis, ICP was also applied to further confirm the introduction of

AAPBA. According to the result of ICP, the element B is 10.2 mg/L in 0.1 g/L microgel. This result indicated that AAPBA has been successfully incorporated into the units of microgel.

Fig. S3 The morphology of fabricated microgels was observed by transmitting polarized microscope at 1 mg/mL.

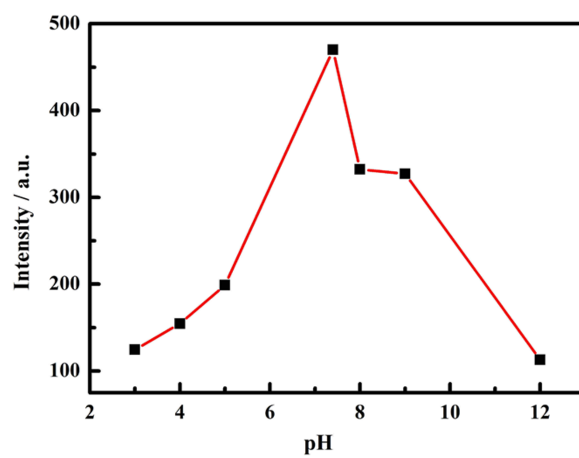

Fig. S4 Fluorescent intensity changes as pH value varies.

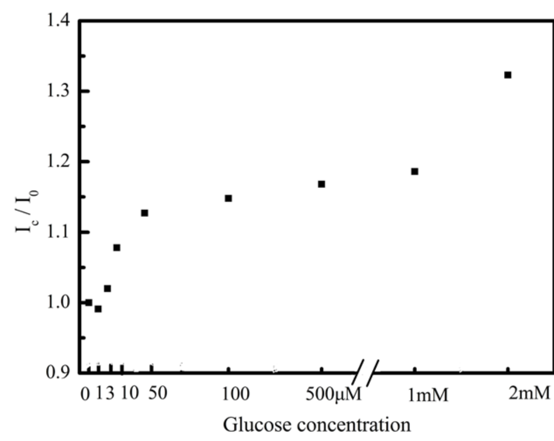

Fig. S5 The ability in detecting glucose was evaluated under physiological condition.

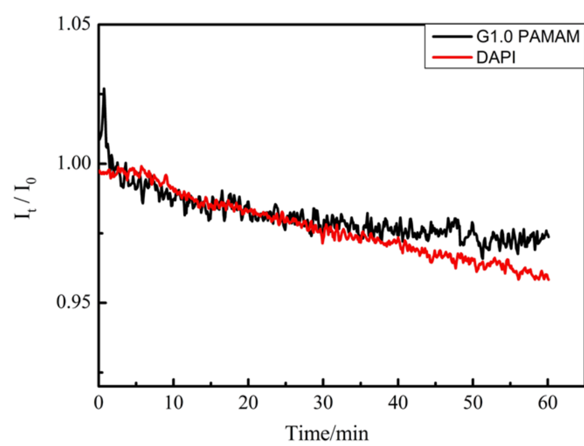

Fig. S6 The ability of G1.0 PAMAM and DAPI in anti-photobleaching was investigated.

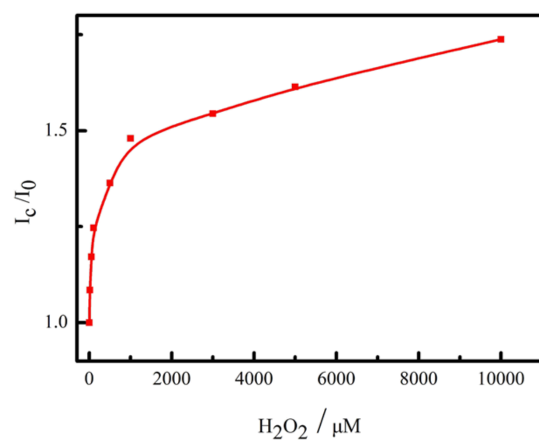

Fig. S7 Relevant fluorescent intensity was investigated as the concentration of H_2O_2 increasing.

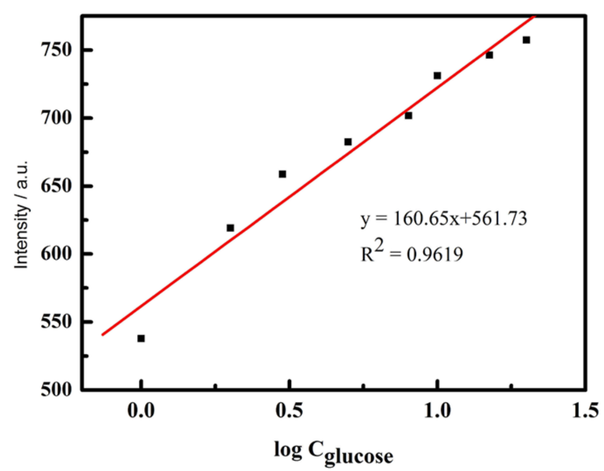

Fig. S8 Glucose response of fabricated microgels in the presence of different glucose concentration as calibration curves.

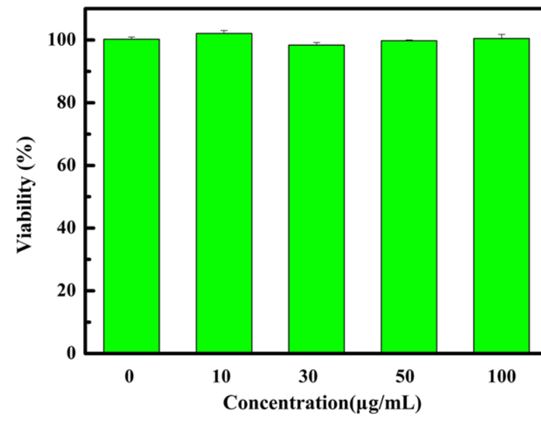

Fig. S9 *In vitro* cytotoxicity tests of G1.0 PAMAM-functionalized microgels. The data are presented as mean ± SD (n = 5).

Table S1 The swelling ratio of microgels changes as glucose concentration increases.

Glucose (mM)	0	5	10	20
Dh (nm)	239	334	381	477
Sr[a]	1.0	1.40	1.59	1.99

a swelling ratio (Sr) = $\frac{D_{h,m}}{D_{h,o}}$

D $_{h,m}$ represents hydrodynamic diameter in certain glucose concentration; D $_{h,0}$ represents micrgels diameter without glucose

Table S2 Response time of microgel in reading glucose evaluated under physiological condition.

Glucose (mM)	1	5	10	20
Response time (s)	5.91	4.45	3.05	2.85

Table S3 Formulation used in artificial tear fluid.

Component	Concentration
Sodium bicarbonate	26 mM
Sodium chloride	100 mM
Potassium chloride	16 mM
Urea	5 mM
Ammonia chloride	3 mM
Lactic acid	2.5 mM
Pyruvic acid	0.2 mM
Citric acid	31 µM
Vitamin C	8 µM
Albumins	3.94 g/L
γ-Globulins	2.75 g/L
Lysozyme	1.7 g/L